European Radiology (2019) 29:1203–1210
https://doi.org/10.1007/s00330-018-5615-8

ONCOLOGY

Amid proton transfer (APT) and magnetization transfer (MT) MRI contrasts provide complimentary assessment of brain tumors similarly to proton magnetic resonance spectroscopy imaging (MRSI)

Changliang Su[1] · Lingyun Zhao[1] · Shihui Li[1] · Jingjing Jiang[1] · Kejia Cai[2] · Jingjing Shi[1] · Yihao Yao[1] · Qilin Ao[3] · Guiling Zhang[1] · Nanxi Shen[1] · Shan Hu[1] · Jiaxuan Zhang[1] · Yuanyuan Qin[1] · Wenzhen Zhu[1]

Received: 9 January 2018 / Revised: 18 May 2018 / Accepted: 18 June 2018 / Published online: 13 August 2018

Abstract

Objectives Using MRSI as comparison, we aimed to explore the difference between amide proton transfer (APT) MRI and conventional semi-solid magnetization transfer ratio (MTR) MRI, and to investigate if molecular APT and structural MTR can provide complimentary information in assessing brain tumors.

Methods Seventeen brain tumor patients and 17 age- and gender-matched volunteers were included and scanned with anatomical MRI, APT and MT-weighted MRI, and MRSI. Multi-voxel choline (Cho) and N-acetylaspartic acid (NAA) signals were quantified from MRSI and compared with MTR and $MTR_{asym(3.5ppm)}$ contrasts averaged from corresponding voxels. Correlations between contrasts were explored voxel-by-voxel by pooling values from all voxels into Pearson's correlation analysis. Differences in correlation coefficients were tested with the Z-test (set at $p<0.05$).

Results APT and MT provide good contrast and quantitative parameters in tumor imaging, as do the metabolite (Cho and NAA) maps. $MTR_{asym(3.5ppm)}$ significantly correlated with MTR (R=-0.61, $p<0.0001$), Cho (R=0.568, $p<0.0001$) and NAA (R=-0.619, $p<0.0001$) in tumors, and MTR also significantly correlated with Cho (R=-0.346, $p<0.0001$) and NAA (R=0.624, $p<0.0001$). In healthy volunteers, $MTR_{asym(3.5ppm)}$ was non-significantly correlated with MTR (R=-0.049, $p=0.239$), Cho (R=0.030, $p=0.478$) and NAA (R=-0.083, $p=0.046$). Significant correlations were found among MTR with Cho (R=0.199, $p<0.0001$) and NAA (R=0.263, $p<0.0001$) in the group of healthy volunteers with lower correlation R values than those in tumor patients.

Conclusions APT and MT could provide independent and supplementary information for the comprehensive assessment of molecular and structural changes due to brain tumor cancerogenesis.

Key Points

- *$MTR_{asym(3.5ppm)}$ positively correlated with Cho while negatively with NAA in tumors.*
- *MTR positively correlated with NAA while negatively with Cho in tumors.*
- *Combining APT/MT provides molecular and structural information similarly to MRSI.*

Keywords Amide proton transfer · Magnetization transfer · Magnetic resonance spectroscopic imaging · Brain tumor

✉ Wenzhen Zhu
zhuwenzhen8612@163.com

[1] Department of Radiology, Tongji Hospital, Tongji Medical College, Huazhong University of Science and Technology, No. 1095 JieFang Avenue, Hankou, Wuhan 430030, People's Republic of China

[2] The Department of Radiology and Bioengineering, College of Medicine, University of Illinois at Chicago, Chicago, IL, USA

[3] Department of Pathology, Tongji Hospital, Tongji Medical College, Huazhong University of Science and Technology, No. 1095 JieFang Avenue, Hankou, Wuhan 430030, People's Republic of China

Abbreviations

APT	Amide proton transfer
MRSI	Magnetic resonance spectroscopy imaging
MT	Magnetization transfer
MTR	Conventional magnetization transfer ratio
$MTR_{asym(3.5ppm)}$	Asymmetrical magnetization transfer ratio at 3.5 ppm

Introduction

MRI shows great advantages by providing remarkable soft-tissue contrasts, and contrast-enhanced T_1-weighted MRI images have been shown to significantly improve diagnostic accuracy in cancer clinics [1, 2]. Considering the side effects of gadolinium on renal disease patients [3] and its long-term potential side effects on brain [4, 5], non-invasive MRI imaging methods are still highly desirable.

Nowadays, many advanced MRI techniques can be used to characterize tissue properties and produce excellent contrasts reflecting pathophysiological information at structural, metabolic and molecular levels, among which chemical shift imaging (CSI) or proton magnetic resonance spectroscopic imaging (MRSI) has demonstrated its value. Based on the discrepancy of chemical shift of ^{1}H proton in various metabolites, proton magnetic resonance spectroscopic imaging (MRSI) showed its strength in non-invasively mapping metabolites of the human brain [6–8]. For instance, due to accelerated membrane synthesis of rapidly dividing cancer cells, Cho is elevated in tumors. Hence, Cho serves as a biomarker for tumor metabolic rate. On the other hand, NAA is generally treated as a neuronal marker found only in neurons and most brain tumors of neuronal origin, and it is reduced or absent in tumors [7]. Since NAA is highly associated with neurons, it is treated as a biomarker reflecting structural changes or neuronal integrity. Given that both Cho and NAA can be quantified with MRSI, MRSI may be utilized for the assessment of brain tumor cancerogenesis at both metabolic and structural levels.

Conventional magnetization transfer imaging (MT) could indirectly map structural macro-molecules with very short T_2, which are invisible in conventional MRI. With non-selective saturation pulse, conventional magnetization transfer ratio (MTR) imaging could detect semi-solid macromolecules of organisms such as protein, lipid and nucleic acid. Previous investigations revealed MTR could contribute to exploring characteristics of brain tumors at pre-surgery stage [9] and estimate myelination in the developing brain [10, 11]. However, MTR by itself suffers from insufficient performance for glioma classification [12]. Recently it has been shown that the asymmetrical magnetization transfer ratio imaging at 3.5 ppm ($MTR_{asym(3.5ppm)}$) or amide proton transfer (APT) MRI allows the detection of intercellular mobile proteins and peptides [13]. Numerous studies have explored its value in assessing the core area of tumors [13], predicting histopathological grades of adult gliomas [14] and distinguishing pseudo-progression from true progression [15].

Given that MTR provides information on structural molecules and APT on functional mobile metabolites, we aimed to investigate if the combination of these two imaging methods may provide complimentary information for the assessment of brain tumor. MRSI with the capacity of showing metabolites reflecting both metabolic and structural tissue information are compared. The metabolite signals from MRSI are used to correlate to MTR and MTR asymmetry-based APT contrast.

Patients and methods

Patients

This prospective study was performed using protocols approved by the Institutional Ethics Committee. Informed consent was obtained before MRI scanning. Seventeen brain tumor patients and 17 age- and gender-matched healthy volunteers were included. Healthy volunteers reported no tumor history or other neurological diseases. In the tumor patients, three cases were glioblastomas (grade IV), four anaplastic astrocytomas (grade III), five astrocytomas (three grade II and two grade I), one oligodendroglioma (grade II), two meningiomas (grade I) and two diffuse large B-cell lymphomas. In total, there were 12 primary tumors, and five recurrent gliomas. The diagnosis was confirmed by either post-surgery pathological examination or follow-up MRI. The tumor and healthy groups were age-matched (42.47±11.23 years vs. 42.29±11.11 years, p=0.96).

Data acquisition

MRI scanning was conducted with a 3.0 T GE MR 750 system (GE Healthcare, Waukesha, WI, USA). The imaging protocol included transverse T_1- and T_2-weighted images (WI), T_2 fluid-attenuated inversion recovery (T_2-FLAIR) and contrast-enhanced T_1-weighted images (T_1C). All sequences had the same thickness/spacing (5/1.5 mm) and field of view (FOV, 240 × 240 mm^2) with 20 slices that covered the entire brain. The acquired images were used as anatomical references for the prescription of APT, MT and MRSI scanning.

For MRSI, two-dimensional, multi-voxel ^{1}H imaging based on the point-resolved spectroscopy pulse sequence (PRESS) for volume of interest (VOI) was applied. Water suppression module included three consecutive chemical shift selective (CHESS) pulses with crush gradients in different axes. The scan plane was centred on the maximum cross-section of tumor patients or centrum semiovale in healthy volunteers. The parameters were as follows: TR=1,000 ms, TE=144 ms, FOV 240 × 240 mm^2, 18 × 18 phase-encoding steps, slice thickness of 14 mm, NEX=0.8, voxel dimension of 7.5 × 7.5 × 14 mm^3, scanning time 4 min and 20 s. The VOIs were carefully placed to avoid hemorrhage, calcification, cystic and necrotic areas, large vessels and strong interference caused by subcutaneous fats and lipids of skull. Saturation slabs were applied in six directions to reduce potential artefacts.

Z-spectra were collected across the same slices as MRSI for constructing APT and MTR contrast maps before T_1C to avoid potential interference due to injection of gadolinium. RF saturation pulse train consisted of four pulses at 2μT amplitude and for 400-ms duration each. The parameters were as follows: TR/TE=3,000/22.6 ms, matrix size of 128 × 128, FOV of 240 × 240 mm^2, 2 NEX, and slice thickness of 5 mm. Data were acquired with a list of saturation frequencies: +15.6, ± 6, ±5, ± 4.5, ± 4, ±3.75, ±3.5, ±3.25, ±3, ±2.5, ±2, ±1.5, ±1, ±0.75, ± 0.5, ±0.25, 0 ppm and one image (S_0) without saturation. The scanning time for Z-spectrum was 3 min 18 s.

Data processing

Raw data were transferred to GE AW4.6 workstation and reconstructed with its Functool software. MTR maps were calculated at +15.6 ppm saturation offset (MTR= (S_0 − $S_{saturation}$)/S_0), while $MTR_{asym(3.5ppm)}$ was calculated at +3.5 ppm as described in the literature [17]. Spectra analysis for MRSI data was also performed with Functool. The processing included filtering to reduce noise, zero-filling, water signal suppression, Fast Fourier Transformation, and baseline and phase corrections. The quantification of metabolite peaks corresponding to Cho and NAA was performed with curve fitting. The analysis procedures were visually and concisely summarized in Fig. 1. With the help of anatomical MRI, we selected voxels that were fully located in the tumor parenchyma by an experienced radiologist, and voxels with normal brain tissues and necrotic areas were excluded. Values of parameters were calculated as the mean value of each targeted voxel.

Statistical analysis

All values are expressed as mean ± standard deviation. To explore the relationship between $MTR_{asym(3.5ppm)}$, MTR and MRSI (Cho and NAA), Pearson's correlation analysis was adopted at the group level with all the voxels of interest from tumor patients or healthy volunteers. To confirm the influence of cancerogenesis on the correlations between APT, MT and MRSI (Cho, NAA), we compared the correlation coefficients in inter- and intra-group correlations using a statistical Z test. For inter-group comparison, correlation coefficients obtained from the patient or healthy groups were compared. For intra-group comparison, individual correlation coefficients were compared within each group of patients or healthy subjects. The statistical results are summarized in Tables 2 and 3. A default *p*-value of 0.05 for significant difference was used for all two-tailed tests. Statistical analyses were carried out using SPSS, IBM 19 or Prism 5.0 GraphPad software.

Results

APT, MT and MRSI differentiate tumors from normal tissue

APT, MT and Cho and NAA maps from MRSI provided distinctive tumor contrasts from normal brain tissues. $MTR_{asym(3.5ppm)}$ in tumors was significantly higher than that in normal tissues, so was Cho as a biomarker of tumor proliferation (Table 1). Conversely, MTR in tumors was significantly lower than that in healthy tissue; and NAA shared a similar contrast to MTR between tumor and normal brain tissue (Table 1). Representative cases of astrocytoma (Grade II) and anaplastic astrocytoma (Grade III) are shown in Figs. 2 and 3.

Correlations between APT, MT and MRSI (Cho and NAA) contrasts

A total of 428 voxels were included in the analysis of brain tumor patients, and 582 voxels in healthy volunteers. $MTR_{asym(3.5ppm)}$ displayed a negative correlation with MTR in brain tumor patients (R=-0.61, $p<0.0001$), while no significant correlation was observed in healthy volunteers (R = -0.049, $p=0.239$, Fig. 4). Moreover, $MTR_{asym\ (3.5ppm)}$ increased with the increase in Cho (R=0.568, $p<0.0001$) and decreased with the reduction of NAA (R=-0.619, $p<0.0001$); however, no significant correlation was obtained in healthy volunteers (Fig. 4). MTR decreased when the Cho signal increased (R=-0.346, $p<0.0001$) and increased with the increase in NAA (R=0.624, $p<0.0001$) in tumors. In healthy volunteers, correlations were weaker between MTR and Cho (R=0,199, $p<0.0001$) and between MTR and NAA (R=0.263, $p<0.0001$) (Fig. 4). Representative cases of those metabolites with scatter plots in individual levels are also displayed in Figs. 2 and 3.

Cross-group comparisons of parameter correlations within tumor patients and healthy volunteers

In inter-group comparisons, the correlations between APT, MT and MRSI (Cho and NAA) in tumors were obviously stronger than those in normal brain tissues, as shown in Fig. 4. The correlation coefficients of $MTR_{asym(3.5ppm)}$ with Cho and $MTR_{asym(3.5ppm)}$ with NAA in tumor patients were obviously retrospectively larger than those in healthy volunteers (for Cho: 0.568 vs. 0.03, z=9.62, $p<0.0001$; for NAA: -0.619 vs. -0.083, z=-10.02, $p<0.0001$). Although the correlations of MTR with MRSI parameters (Cho, NAA) were all significant in the two groups, as displayed in Fig. 4, the Z-test confirmed evident differences of those correlations between the two groups with statistical significance (with Cho: -0.346 vs. 0.199, Z=-8.808, $p<0.0001$; with NAA: 0.624 vs. 0.263,

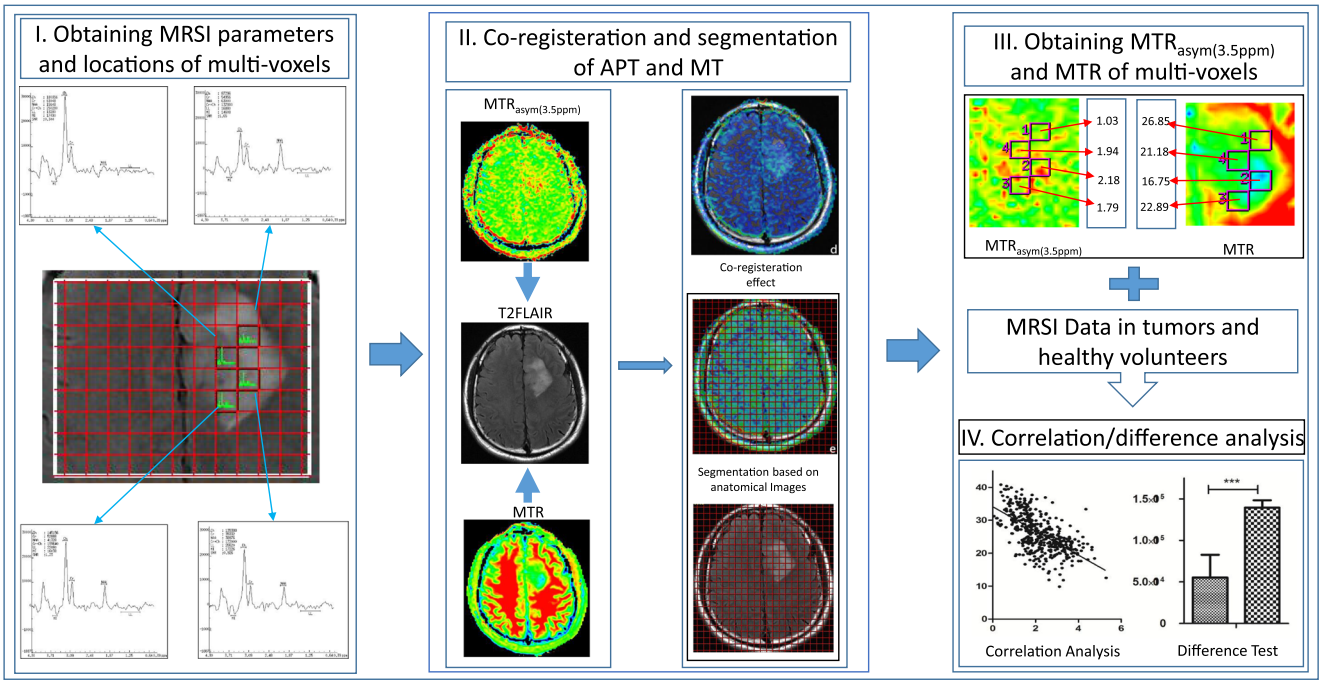

Fig. 1 Flowchart showing the course of data analysis. **From left to right: I.** MRSI parameters (Cho and NAA) and location information of multi-voxels were obtained. **II.** $MTR_{asym(3.5ppm)}$ and MTR contrast maps were automatically matched with anatomical images and segmented to multi-regions corresponding to the locations of MRSI multi-voxels by the grid came with the Functool. **III.** The value of $MTR_{asym(3.5ppm)}$ and MTR were calculated as the mean value of each voxel. **IV.** $MTR_{asym(3.5ppm)}$ and MTR were analysed with Pearson's correlation analysis within two groups, and the correlation coefficients were tested by the Z-test

Z=7.238, $p<0.0001$), indicating a stronger correlation due to tumor cancerogenesis. These results are concisely summarized in Table 2.

For intra-group comparisons, significant correlations between APT, MT and MRSI (Cho and NAA) were found in tumor patients, while non-significant correlations were found in healthy subjects (for details, please see Table 3).

Discussion

We have demonstrated in this study that MTR and APT provide structural and metabolic contrasts that correlate with MRSI signals reflecting structural and metabolic tissue information, particularly in tumors. Combining APT and MT MRI could offer mutually complementary information and serve as a powerful tool for the diagnosis and characterization of brain tumors.

Significant correlations between MTR, $MTR_{asym(3.5ppm)}$ and MRSI (Cho, NAA) in tumors

In age- and gender-matched brain tumor patients and healthy volunteers, we observed significant correlations between $MTR_{asym(3.5ppm)}$, MTR and MRSI (Cho, NAA) contrasts in brain tumors. The rapid tumorous growth accompanies a high proliferation rate of tumor cells, resulting in the increase of mobile proteins and tumor cell density [19]. Previous studies have shown that APT detects cellular endogenous proteins and peptides, providing good contrast for brain tumors [13, 16, 18]. The increased mobile proteins and reduced cancer pH lead to an increase in APT signal intensities. On the other hand, the increased cell density is accompanied by the

Table 1 The manifestation of MRSI, APT and MT parameters in tumor patients and healthy volunteers

	Tumor patients	Healthy volunteers	T-value	*p*-value
Cho*	107,913.00±19,161.49	68,610.68±6,757.69	-7.76	$p<0.0001$
NAA*	55,270.12±27,354.49	139,463.50±6,984.55	11.73	$p<0.0001$
$MTR_{asym(3.5ppm)}$(%)	2.26±0.59	0.82±0.29	-8.73	$p<0.0001$
MTR(%)	25.60±3.32	36.64±1.96	11.54	$p<0.0001$

The mean values of four parameters in tumors significantly differed from those in the normal brain

* The unit for Cho and NAA is a.u. (arbitrary unit)

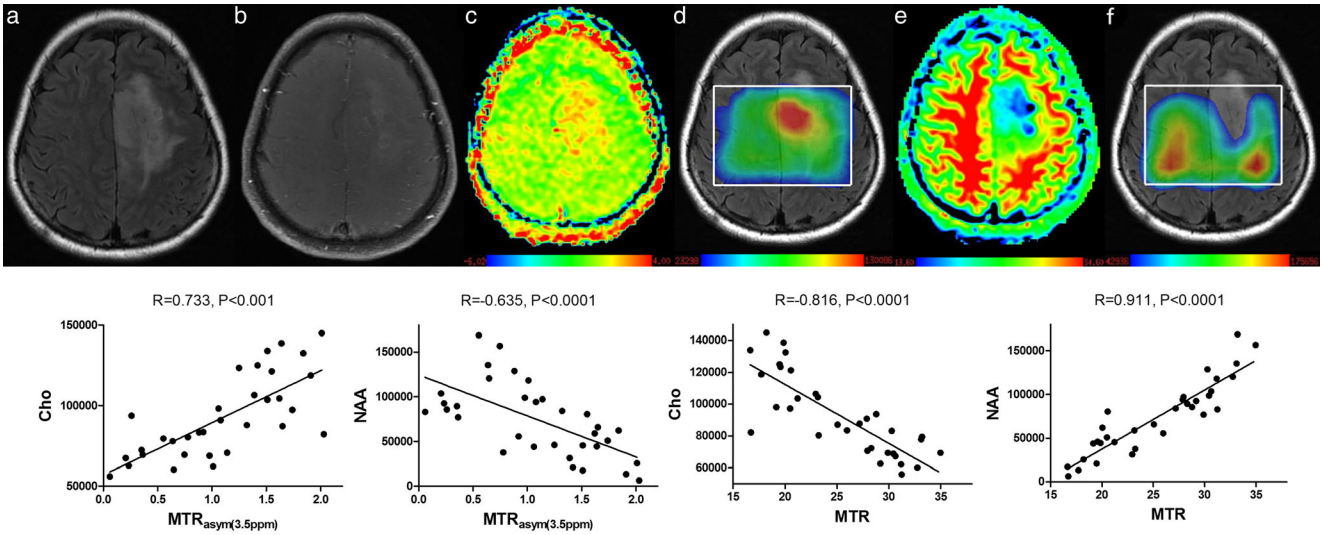

Fig. 2 A representative case of astrocytoma (grade II). **First row:** T_2 FLAIR (a); b, T_1C(b); $MTR_{asym(3.5ppm)}$ (c),Cho(d), MTR (e) and NAA (f). $MTR_{asym(3.5ppm)}$ map and Cho map exhibited good consistency in depicting the hot spot of the tumor. MTR and NAA matched well with each other in manifesting areas affected by tumor growth. **Second row:** Scatter plots of APT, MT and MRSI parameters. The strong correlations were revealed by scatter plots and R of MTR with NAA reached up to 0.9

addition of cell membranes that contain many choline components, thus leading to an elevation in Cho signals. MTR is mainly contributed by the predominant interaction between free liquid water and macromolecules. Free protons in lesions with a high water content or reduced immobile macromolecules concentration are believed to be less saturated by off-resonance irradiation, which leads to lower MTRs [20].The rapidly dividing cancer cells result in destruction of normal brain tissues, thus leading to obvious losses of neurons and low NAA peaks [6]. Hence, the correlations between $MTR_{asym(3.5ppm)}$, MTR and MRSI (Cho and NAA) in tumors when compared with normal brain tissues, as observed in our study, is reasonable. Numerous studies have focused on APT, MT and MRSI in brain tumors [7, 14, 16, 17, 21], yet only few studies have made a thorough investigation of the correlations between those imaging contrasts. This study has filled this gap. Previous studies have reported MTR and APT as two promising, complementary imaging methods for the assessment of brain development in pediatrics and neonatal care [11, 22]. Our research further demonstrated that MTR and APT

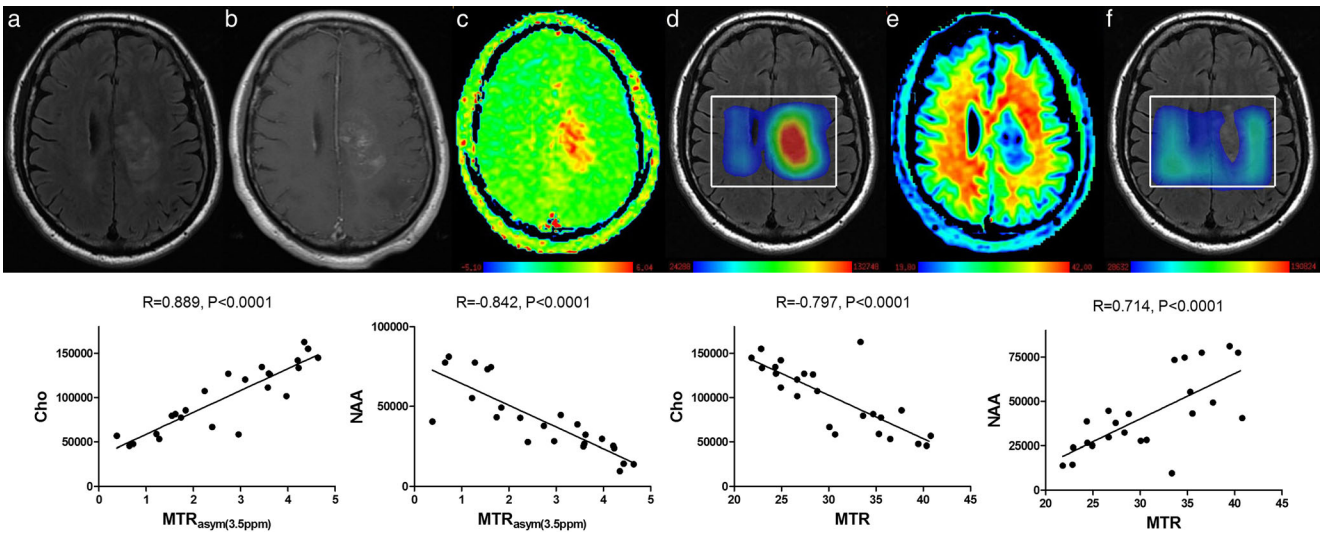

Fig. 3 A representative case of anaplastic astrocytoma (grade III). **First row:** T_2 Flair (a); b, T_1C (b); the colour maps of $MTR_{asym(3.5ppm)}$ (c),Cho(d), MTR (e) and NAA (f). The $MTR_{asym(3.5ppm)}$ map showed good contrast in tumor areas depicted by high intensities in T_2 Flair and contrast enhancement, which also exhibited good consistency with the hot spot of Cho. The MTR map exhibited decreased MTR in solid tumor part and matched well with the low concentration of NAA imaged in the NAA colour map, which may reflect the neuron damage caused by tumor growth. **Second row:** The scatter plots of APT, MT and Cho, NAA. The correlations were strong, even in a high-grade glioma

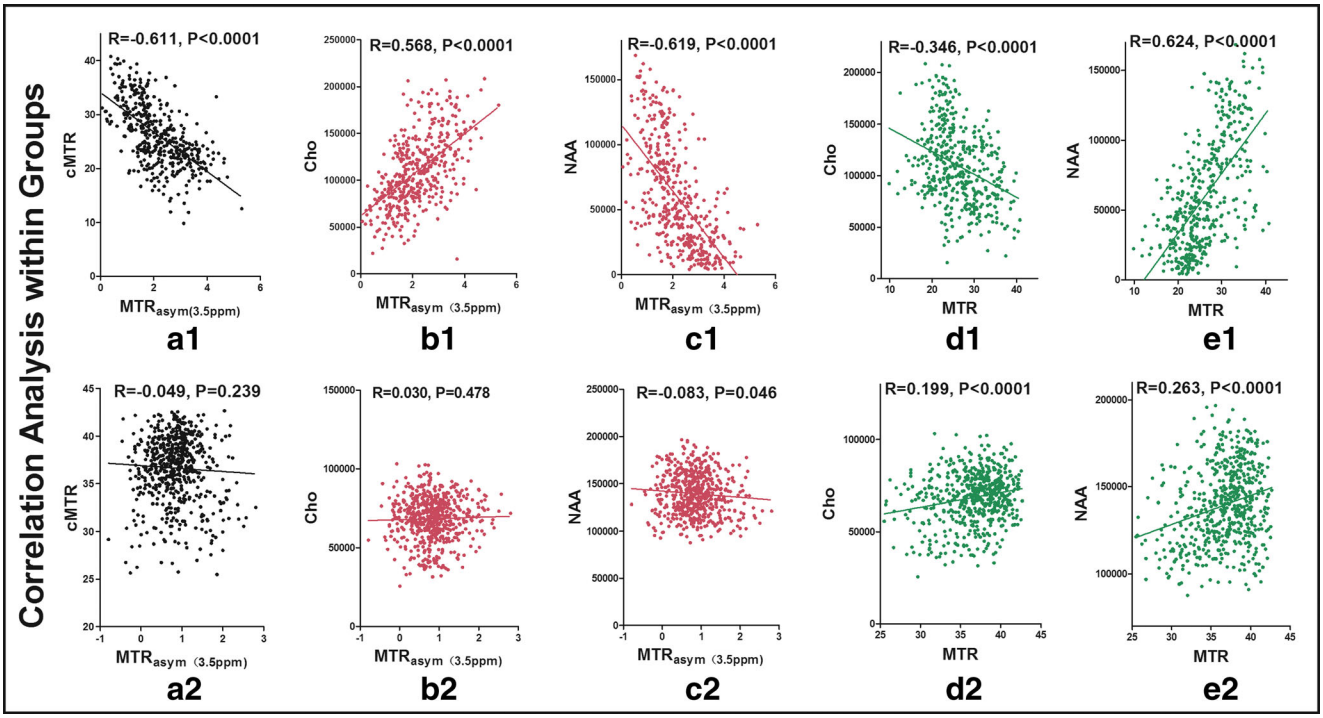

Fig. 4 Correlation analysis between $MTR_{asym(3.5ppm)}$, MTR and MRSI (Cho, NAA). 428 voxels in tumors and 582 voxels in volunteers were included. $MTR_{asym(3.5ppm)}$ significantly correlated with MTR values (**a1**) in tumors and non-significantly in volunteers (**a2**). In tumors, $MTR_{asym(3.5ppm)}$ significantly increased with Cho (**b1**) and decreased with NAA (**c1**). On the other hand, MTR decreased with Cho (**d1**) and escalated with NAA (**e1**). In volunteers, there were few correlations between $MTR_{asym(3.5ppm)}$ and Cho, NAA (**b2** and **c2**). However, weak but significant correlations existed between MTR and Cho, NAA (**d2** and **e2**)

supply complimentary information in tumor imaging at both structural and metabolic levels, allowing more comprehensive assessment of brain tumors.

The difference between APT and MTR

With voxel-by-voxel correlation analysis, different correlation patterns between $MTR_{asym(3.5ppm)}$, MTR with MRSI (Cho, NAA) were observed, providing clinical evidence for the different contrast mechanisms of APT and MT. With the selective radiofrequency at 3.5ppm, $MTR_{asym(3.5ppm)}$ predominantly reflects an amide proton transfer effect, which maps total amide proton concentrations of cellular mobile proteins and peptide, manifesting excellent contrasts [13, 23]. Due to relatively low concentrations of mobile proteins and peptides, APT is not supposed to be sensitive to structural macromolecules in the tissues [13]. On the contrary, MT MRI reflects the amount and complexity of structural macromolecules [24], especially for immobile macromolecules in tissue [25], providing excellent anatomical details for brain tissues. With a non-selective radiofrequency irradiation, the MT effect is theoretically considered on the base of magnetization exchange between free and bound water protons. In the clinical applications, owing to its vulnerability to the concentration, chemical structure and mobility of myelin constituents [26, 27], MTR might be sensitive in reflecting brain tissue destruction caused by brain diseases [20, 28]. However, it is still not specific enough to significantly differentiate between low/high grade

Table 2 Inter-group comparisons of correlation coefficients in tumors and normal brains

	MRSI	Tumors	Normal brains	Z-value	*p*-value
$MTR_{asym(3.5ppm)}$ (%)	vs. Cho	0.568	0.03	9.62	$p<0.0001$*
	vs. NAA	-0.619	-0.083	-10.02	$p<0.0001$*
MTR (%)	vs. Cho	-0.346	0.199	-8.808	$p<0.0001$*
	vs. NAA	0.624	0.263	7.238	$p<0.0001$*

The comparisons of correlation coefficients in brain tumor patients and healthy volunteers were implemented with the Z-test. The differences in correlations of $MTR_{asym(3.5ppm)}$ vs. Cho, NAA was significant both in tumor patients and in healthy volunteers, as was that of MTR vs. Cho, NAA. These results indicate the different and significant correlations between metabolites in tumors and in normal brain tissues

$p<0.05$

Table 3 Intra-group comparisons of correlation coefficients in tumors and normal brains

Parameters	Groups	vs. Cho	vs. NAA	Z-value	*p*-value
$MTR_{asym(3.5ppm)}$ (%)	Tumors	0.568	-0.619	19.94	$p<0.0001$*
	Normal brains	0.03	-0.083	1.65	0.099
MTR (%)	Tumors	-0.346	0.624	15.93	$p<0.0001$*
	Normal brains	0.199	0.263	-1.15	0.25

Intra-group comparisons were conducted within each group to explore the different correlation significance of $MTR_{asym(3.5ppm)}$ (%) or MTR (%) correlated with the MRSI parameter (vs. Cho, vs. NAA). As shown in the above table, the difference in correlation coefficients obtained from $MTR_{asym(3.5ppm)}$ vs. Cho and $MTR_{asym(3.5ppm)}$ vs. NAA was significant in tumor patients and non-significant in healthy volunteers, and a similar result was also observed in MTR. The comparison also indicated altered correlations among those parameters due to cancerogenesis

$p<0.05$

gliomas and benign/malignant brain tumors [20], which also differsfrom APT. Hence, APT and MTR contribute different pathophysiological aspects of tumors.

Combined APT and MT might serve as useful tool similar to MRSI in assessing brain tumors

A comparison of pathological results [14] and single-voxel ^{1}H-MRS studies [16], $MTR_{asym(3.5ppm)}$ has shown its capability for detecting tumor proliferation, suggesting that APT imaging may serve as an alternative tool for MR spectroscopy. In this study, we provide further evidence to support the relationships between APT, MT and MRSI. With single-voxel MR spectroscopy, heterogeneity of tumors might be underevaluated due to the volume effect. MRSI allows a more precise evaluation of tumor metabolites with higher spatial resolution. Since $MTR_{asym(3.5ppm)}$ and MTR are strongly correlated with Cho and NAA in tumors, combining APT/MT may provide as abundant composition information as MRSI does in the assessment of brain tumors. In addition, producing quantitative metabolite maps from MRSI requires not only a highly homogeneous magnetic field but also extensive experience. Moreover, APT imaging showed comparable diagnostic capability to MR spectroscopy for grading brain tumors, as compared in previous diagnostic testing [29]. Considering the pathophysiological roles of Cho and NAA and the close correlations with APT and MT, combining APT and MT might provide complementary information similar to MRSI (Cho, NAA) in the assessment of tumor structural and metabolic changes.

There are some limitations to this study. First of all, APT, MT and MRSI were scanned in a single representative slice due to technical limitations and restricted scanning time. Secondly, although hundreds of voxels were included in the analysis that could achieve a reliable result in each group correlation analysis, a larger sample size might be more persuasive. In addition, in spite of the persuasive evidence supporting the correlations between multiple imaging contrasts, more pathological and biochemical measurements would be more helpful for validating these image contrasts and assessing tissue structural integrity and metabolites.

Conclusion

In conclusion, APT and MT can provide complimentary contrasts for brain tumors despite their differences in contrast mechanisms. $MTR_{asym(3.5ppm)}$ and MTR correlated with MRSI parameters (Cho, NAA) significantly. Combining $MTR_{asym(3.5ppm)}$ and MTR could supply independent and mutually complementary information in assessing tumor biological behaviours at a molecular level, thus might make it potentially an alternative to MR spectroscopy in imaging brain tumors.

Acknowledgements We thank Bing Wu from GE health for his generous help in data post-processing and advice on the manuscript. We also acknowledge Dr. Yang Fan from General Electric Company (China) for his generous contributions to manuscript revision.

Funding This study has received funding by grants from the National Program of the Ministry of Science and Technology of China during the "12th Five-Year Plan" (ID: 2011BAI08B10) and the National Natural Science Foundation of China (No. 81171308, No. 81570462, No. 81730049 and No. 81401389). This work is also partially supported by NIH NIBIB grant R21-EB023516-02 (Cai).

Compliance with ethical standards

Guarantor The scientific guarantor of this publication is Wenzhen Zhu.

Conflict of interest The authors of this manuscript declare no relationships with any companies whose products or services may be related to the subject matter of the article.

Statistics and biometry No complex statistical methods were necessary for this paper.

Informed consent Written informed consent was obtained from all subjects (patients) in this study.

Ethical approval Institutional Review Board approval was obtained.

Methodology
- Prospective
- Observational
- Performed at one institution

References

1. Ramalho J, Ramalho M, AlObaidy M, Semelka RC (2016) Technical aspects of MRI signal change quantification after gadolinium-based contrast agents' administration. Magn Reson Imaging 34(10):1355–1358
2. Thieme ME, Leeuwenburgh MM, Valdehueza ZD et al (2014) Diagnostic accuracy and patient acceptance of MRI in children with suspected appendicitis. Eur Radiol 24(3):630–637
3. Deo A, Fogel M, Cowper SE (2007) Nephrogenic systemic fibrosis: a population study examining the relationship of disease development to gadolinium exposure. Clin J Am Soc Nephrol 2(2):264–267
4. Kuno H, Jara H, Buch K, Qureshi MM, Chapman MN, Sakai O (2017) Global and regional brain assessment with quantitative MR imaging in patients with prior exposure to linear gadolinium-based contrast agents. Radiology 283(1):195–204
5. Kanda T, Oba H, Toyoda K, Kitajima K, Furui S (2016) Brain gadolinium deposition after administration of gadolinium-based contrast agents. Jpn J Radiol 34(1):3–9
6. Howe FA, Barton SJ, Cudlip SA et al (2003) Metabolic profiles of human brain tumors using quantitative in vivo 1H magnetic resonance spectroscopy. Magn Reson Med 49(2):223–232
7. Howe FA, Opstad KS (2003) 1H MR spectroscopy of brain tumours and masses. NMR Biomed 16(3):123–131
8. Nelson SJ (2003) Multivoxel magnetic resonance spectroscopy of brain tumors. Mol Cancer Ther 2(5):497–507
9. Okumura A, Takenaka K, Nishimura Y et al (1999) The characterization of human brain tumor using magnetization transfer technique in magnetic resonance imaging. Neurol Res 21(3):250–254
10. van Buchem MA, Steens SC, Vrooman HA et al (2001) Global estimation of myelination in the developing brain on the basis of magnetization transfer imaging: a preliminary study. AJNR Am J Neuroradiol 22(4):762–766
11. Zhang H, Kang H, Zhao X et al (2016) Amide Proton Transfer (APT) MR imaging and Magnetization Transfer (MT) MR imaging of pediatric brain development. Eur Radiol 26(10):3368–3376
12. Kurki T, Lundbom N, Kalimo H, Valtonen S (1995) MR classification of brain gliomas: value of magnetization transfer and conventional imaging. Magn Reson Imaging 13(4):501–511
13. Zhou J, Lal B, Wilson DA, Laterra J, van Zijl PC (2003) Amide proton transfer (APT) contrast for imaging of brain tumors. Magn Reson Med 50(6):1120–1126
14. Togao O, Yoshiura T, Keupp J et al (2014) Amide proton transfer imaging of adult diffuse gliomas: correlation with histopathological grades. Neuro Oncol 16(3):441–448
15. Ma B, Blakeley JO, Hong X et al (2016) Applying amide proton transfer-weighted MRI to distinguish pseudoprogression from true progression in malignant gliomas. J Magn Reson Imaging 44(2): 456–462
16. Park JE, Kim HS, Park KJ, Kim SJ, Kim JH, Smith SA (2016) Pre- and posttreatment glioma: comparison of amide proton transfer imaging with mr spectroscopy for biomarkers of tumor proliferation. Radiology 278(2):514–523
17. Zhou J, Zhu H, Lim M et al (2013) Three-dimensional amide proton transfer MR imaging of gliomas: Initial experience and comparison with gadolinium enhancement. J Magn Reson Imaging 38(5):1119–1128
18. Wen Z, Hu S, Huang F et al (2010) MR imaging of high-grade brain tumors using endogenous protein and peptide-based contrast. Neuroimage 51(2):616–622
19. Brada M (2001) Pathology and genetics of tumours of the nervous system. Br J Cancer 84(1):148
20. Pui MH (2000) Magnetization transfer analysis of brain tumor, infection, and infarction. J Magn Reson Imaging 12(3): 395–399
21. Kurki T, Lundbom N, Komu M, Kormano M (1996) Tissue characterization of intracranial tumors by magnetization transfer and spin-lattice relaxation parameters in vivo. J Magn Reson Imaging 6(4):573–579
22. Zheng Y, Wang X, Zhao X (2016) Magnetization transfer and amide proton transfer MRI of neonatal brain development. Biomed Res Int 2016:3052723
23. Zhou J, Yan K, Zhu H (2012) A simple model for understanding the origin of the amide proton transfer MRI signal in tissue. Appl Magn Reson 42(3):393–402
24. Gass A, Barker GJ, Kidd D et al (1994) Correlation of magnetization transfer ratio with clinical disability in multiple sclerosis. Ann Neurol 36(1):62–67
25. Henkelman RM, Stanisz GJ, Graham SJ (2001) Magnetization transfer in MRI: a review. NMR Biomed 14(2):57–64
26. Ceckler TL, Wolff SD, Yip V, Simon SA, Balaban RS (1992) Dynamic and chemical factors affecting water proton relaxation by macromolecules. J Magn Reson 98(3):637–645
27. Fralix TA, Ceckler TL, Wolff SD, Simon SA, Balaban RS (1991) Lipid bilayer and water proton magnetization transfer: effect of cholesterol. Magn Reson Med 18(1):214–223
28. Chen JT, Collins DL, Atkins HL, Freedman MS, Arnold DL, Canadian MS/BMT Study Group (2008) Magnetization transfer ratio evolution with demyelination and remyelination in multiple sclerosis lesions. Ann Neurol 63(2):254–262
29. Sakata A, Fushimi Y, Okada T et al (2017) Diagnostic performance between contrast enhancement, proton MR spectroscopy, and amide proton transfer imaging in patients with brain tumors. J Magn Reson Imaging 46(3):732–739